

# Electron-radiation interaction in a Penning trap: beyond the dipole approximation

Ana M. Martins<sup>†</sup>, Stefano Mancini<sup>‡</sup>, and Paolo Tombesi<sup>‡</sup>

<sup>†</sup> *Centro de Física de Plasmas, Instituto Superior Técnico,  
P-1096 Lisboa Codex, Portugal*

<sup>‡</sup> *Dipartimento di Matematica e Fisica and Istituto Nazionale per la Fisica della Materia,  
Università di Camerino, I-62032 Camerino, Italy*

(Received: April 16, 2018)

We investigate the physics of a single trapped electron interacting with a radiation field without the dipole approximation. This gives new physical insights in the so-called geonium theory.

PACS number(s): 03.65.Bz, 42.50.Dv, 12.20.-m

## I. INTRODUCTION

Simple systems like single electron or ion provide a useful tool to investigate the fundamental laws of nature. Hence in the past decades there has been increasing interest on trapping phenomena [1]. It is now routinely possible to trap a single ion [2], and it would allow us to study QED (Quantum Electro-Dynamics) also when the trapped ion interacts with a radiation mode. On the other hand the electron stored in a Penning trap [3] permitted accurate measurements too [4]. This system has been called "geonium atom" since it resembles an hydrogen atom where indeed the binding for the electron is to an external apparatus residing on the earth [5]. The geonium system was recently studied to implement some interesting quantum optics situations, like QND (Quantum Non-Demolition) measurements [6] and the generation of nonclassical states [7].

Here, just after one hundred years from the electron discovery, we would show new interesting quantum features arising on a trapped electron interacting with the radiation field, when no dipole approximation is made.

It is well known that in the geonium system [5] the motion of the electron can be separated into three independent harmonic motions: the axial, cyclotron and magnetron. On the other hand, it is also well established that entangled systems are extremely interesting for many purposes.

In the present work we propose a way of coupling the three harmonic oscillators of the geonium system by simply superposing a radiation field to the trapping fields. More concretely, we show that when the trapped electron oscillates in a standing wave field, there could be linear, or nonlinear coupling among the axial motion and the other ones; although, in particular we will only consider the axial-cyclotron interaction. Hence, we shall present the more immediate consequences of such an entanglement, like indirect measurements on the cyclotron mode, then we shall investigate the generation of nonclassical features. Moreover, the analysis in all cases will be performed by taking into account the environmental effects as well.

The paper is organized as follow: Section II is devoted to the description of the model. The first order coupling (linear) between axial and cyclotron motion is considered in Section III, while in Section IV the second order coupling is discussed. In Section V we further discuss the possibility of generating nonclassical states. Finally, we present conclusions.

## II. THE MODEL

The geonium system consists [5] of an electron of charge  $e$  and mass  $m_0$  moving in a uniform magnetic field  $\mathbf{B}$ , along the positive  $z$  axis, and a static quadrupole potential

$$\hat{V} = V_0 \frac{\hat{x}^2 + \hat{y}^2 - 2\hat{z}^2}{4d^2}, \quad (1)$$

where  $d$  characterizes the dimension of the trap and  $V_0$  is the potential applied to the trap electrodes [5].

In this work, in addition to the usual trapping fields, we embed the trapped electron in a radiation field of vector potential  $\hat{\mathbf{A}}_{ext}$ . To simplify our presentation, we assume the *a priori* knowledge of the electron spin [8]. Neglecting all spin-related terms, the Hamiltonian for the trapped electron can then be written as the quantum counterpart of the classical Hamiltonian

$$\hat{H} = \frac{1}{2m_0} \left[ \hat{\mathbf{p}} - \frac{e}{c} \hat{\mathbf{A}} \right]^2 + e\hat{V}, \quad (2)$$

where  $c$  is the speed of light, and

$$\hat{\mathbf{A}} = \frac{1}{2} \hat{\mathbf{r}} \wedge \mathbf{B} + \hat{\mathbf{A}}_{ext}, \quad (3)$$

where  $\hat{\mathbf{r}} \equiv (\hat{x}, \hat{y}, \hat{z})$  and  $\hat{\mathbf{p}} \equiv (\hat{p}_x, \hat{p}_y, \hat{p}_z)$  are respectively the position and the conjugate momentum operators of the electron.

The motion of the electron in absence of the external field  $\hat{\mathbf{A}}_{ext}$  is the result of the motion of three harmonic oscillators [5]: the cyclotron, the axial and the magnetron, which are well separated in the energy scale (GHz, MHz and kHz respectively). This can be easily understood by introducing the ladder operators

$$\hat{a}_z = \sqrt{\frac{m_0\omega_z}{2\hbar}} \hat{z} + i \sqrt{\frac{1}{2\hbar m_0\omega_z}} \hat{p}_z \quad (4)$$

$$\hat{a}_c = \frac{1}{2} \left[ \sqrt{\frac{m_0\omega_c}{2\hbar}} (\hat{x} - i\hat{y}) + \sqrt{\frac{2}{\hbar m_0\omega_c}} (\hat{p}_y + i\hat{p}_x) \right] \quad (5)$$

$$\hat{a}_m = \frac{1}{2} \left[ \sqrt{\frac{m_0\omega_c}{2\hbar}} (\hat{x} + i\hat{y}) - \sqrt{\frac{2}{\hbar m_0\omega_c}} (\hat{p}_y - i\hat{p}_x) \right] \quad (6)$$

where the indexes  $z$ ,  $c$  and  $m$  stand for axial, cyclotron and magnetron respectively. The above operators obey the commutation relation  $[\hat{a}_i, \hat{a}_i^\dagger] = 1$ ,  $i = z, c, m$ . The angular frequencies are given by

$$\omega_z = \sqrt{\frac{eV_0}{m_0cd^2}}; \quad \omega_c = \frac{eB}{m_0c}; \quad \omega_m \approx \frac{\omega_z^2}{2\omega_c}. \quad (7)$$

So, when  $\hat{\mathbf{A}}_{ext} = 0$ , the Hamiltonian (2) simply reduces to

$$\hat{H} = \hbar\omega_z \left( \hat{a}_z^\dagger \hat{a}_z + \frac{1}{2} \right) + \hbar\omega_c \left( \hat{a}_c^\dagger \hat{a}_c + \frac{1}{2} \right) - \hbar\omega_m \left( \hat{a}_m^\dagger \hat{a}_m + \frac{1}{2} \right). \quad (8)$$

Instead, when the external radiation field is a standing wave along the  $z$  direction (with frequency  $\Omega$  and wave vector  $k$ ) and circularly polarized in the  $x - y$  plane [9], we have

$$\hat{\mathbf{A}}_{ext} = (-i [\alpha e^{i\Omega t} - \alpha^* e^{-i\Omega t}] \cos(k\hat{z} + \phi), [\alpha e^{i\Omega t} + \alpha^* e^{-i\Omega t}] \cos(k\hat{z} + \phi), 0). \quad (9)$$

In such a case, and for frequencies  $\Omega$  close to  $\omega_c$ , we can neglect the slow magnetron motion, and the Hamiltonian (2) becomes

$$\begin{aligned} \hat{H} &= \hbar\omega_z \left( \hat{a}_z^\dagger \hat{a}_z + \frac{1}{2} \right) + \hbar\omega_c \left( \hat{a}_c^\dagger \hat{a}_c + \frac{1}{2} \right) \\ &+ \hbar [\epsilon^* \hat{a}_c e^{i\Omega t} + \epsilon \hat{a}_c^\dagger e^{-i\Omega t}] \cos(k\hat{z} + \phi) + \hbar\chi \cos^2(k\hat{z} + \phi) \end{aligned} \quad (10)$$

where

$$\epsilon = |\epsilon| e^{i\varphi} = \left( \frac{2e^3 B}{\hbar m_0^2 c^3} \right)^{1/2} \alpha; \quad \chi = \frac{e^2}{\hbar m_0 c^2} |\alpha|^2, \quad (11)$$

and the phase  $\varphi$  is the phase of the applied radiation field (i.e.  $\arg \alpha$ ). The other phase  $\phi$  defines the position of the center of the axial motion with respect to the standing wave. The third and fourth terms in the right hand side of the Hamiltonian (10) describe the nonlinear interaction between the trapped electron and the standing wave which gives rise to a coupling between the axial and the cyclotron motion, whose effect will be analyzed in the next sections. In the usual Penning traps the quantity  $k\langle \hat{z} \rangle$  can reach values up to  $\approx 0.1$  [5], when  $\Omega \approx \omega_c$ . This leads us to explore the physics beyond the usual dipole approximation for the cosine term in Eq. (10). The cosine factor  $\cos(k\hat{z} + \phi)$  can be split as

$$\cos(k\hat{z} + \phi) = \cos \phi \cos(k\hat{z}) - \sin \phi \sin(k\hat{z}), \quad (12)$$

and two typical situations corresponding to  $\phi = 0$  and  $\phi = \pi/2$  can be easily exploited. By making the usual dipole approximation these two cases correspond to a mere driving term on the cyclotron motion ( $\phi = 0$ ) or to no effect at all ( $\phi = \pi/2$ ).

In the following Sections the behaviour of the trapped electron in these two paradigmatic limits is studied. All the other possible values of  $\phi$  will give rise to combinations of these two cases and can be easily studied.

We further note that the last term in (10) can be neglected since the parameters (11) are such that  $\chi/|\epsilon| \approx |\epsilon|/\omega_c$ .

### III. THE CASE OF $\phi = \pi/2$

In this section we consider the case  $\phi = \pi/2$ . Developing  $\sin(k\hat{z})$  in power series and keeping only the first order term we can approximate the Hamiltonian (10) by

$$\begin{aligned} \hat{H} &= \hbar\omega_z \left( \hat{a}_z^\dagger \hat{a}_z + \frac{1}{2} \right) + \hbar\omega_c \left( \hat{a}_c^\dagger \hat{a}_c + \frac{1}{2} \right) \\ &+ \hbar \left[ \epsilon^* \hat{a}_c e^{i\Omega t} + \epsilon \hat{a}_c^\dagger e^{-i\Omega t} \right] k\hat{z}. \end{aligned} \quad (13)$$

In the case of perfect resonance,  $\Omega = \omega_c$ , and in a frame rotating at that angular frequency we get the solution

$$\hat{z}(t) = \left[ \hat{z}(0) - |\epsilon|k\hat{X}_\varphi \right] \cos(\omega_z t) + \frac{1}{m\omega_z} \hat{p}_z(0) \sin(\omega_z t) + |\epsilon|k\hat{X}_\varphi \quad (14)$$

$$\hat{p}_z(t) = \hat{p}_z(0) \cos(\omega_z t) - m\omega_z \left[ \hat{z}(0) - \sqrt{2}|\epsilon|k\hat{X}_\varphi \right] \sin(\omega_z t) \quad (15)$$

where we have introduced the cyclotron quadrature

$$\hat{X}_\varphi = \frac{\hat{a}_c e^{i\varphi} + \hat{a}_c^\dagger e^{-i\varphi}}{\sqrt{2}}. \quad (16)$$

Equation (15) suggests us an indirect way to determine the probability distribution for the cyclotronic quadrature,  $\mathcal{P}(X_\varphi)$ . We recall that in the geonium system the measurements are performed only on the axial degree of freedom due to the non existence of good detectors in the microwave regime. The oscillating charged particle induces alternating image charges on the electrodes, which in turn cause an oscillating current to flow through an external circuit. The current will be proportional to the axial momentum  $\hat{p}_z$ , hence a measurement of this current will also give the value of the quadrature  $\hat{X}_\varphi$ . Measurements when the standing wave is ‘off’ should be done preventively to set the initial conditions. Then, repeated measurements lead to the desired statistics  $\mathcal{P}(X_\varphi)$ .

If the procedure is further repeated for several values of the phase  $\varphi$ , we obtain the set of marginal probabilities  $\mathcal{P}(X, \varphi)$ , which allows the tomographic imaging of the quantum state of the cyclotron mode [10].

We now consider the effects of the thermal damping through the resistance of the external circuit connected with the measurement apparatus. In such a case the equations of motion for the axial degree of freedom become

$$\frac{d\hat{z}}{dt} = \frac{\hat{p}_z}{m_0}, \quad (17)$$

$$\frac{d\hat{p}_z}{dt} = -\omega_z^2 m_0 \hat{z} - \frac{\gamma_z}{m_0} \hat{p}_z - \sqrt{2}\hbar k |\epsilon| \hat{X}_\varphi + \xi, \quad (18)$$

where the noise term  $\xi(t)$  is that of Johnson noise with expectation values  $\langle \xi(t) \rangle = 0$ , and  $\langle \xi(t)\xi(t') \rangle = 2\gamma_z K_B T \delta(t-t')$ , the damping constant  $\gamma_z$  is proportional to the readout resistor,  $K_B$  is the Boltzmann constant and  $T$  the equilibrium temperature.

By using the Fourier transforms, we immediately obtain

$$\tilde{p}_z(\omega) = \frac{\sqrt{2}\hbar k |\epsilon| \tilde{X}_\varphi(\omega) - \tilde{\xi}(\omega)}{\omega^2 - \omega_z^2 - i\omega\gamma_z/m_0}, \quad (19)$$

hence the correlation

$$\langle \tilde{p}_z(\omega) \tilde{p}_z(-\omega) \rangle = \frac{2(\hbar k |\epsilon|)^2 \langle \tilde{X}_\varphi(\omega) \tilde{X}_\varphi(-\omega) \rangle + \langle \tilde{\xi}(\omega) \tilde{\xi}(-\omega) \rangle}{|\omega^2 - \omega_z^2 - i\omega\gamma_z/m_0|^2}. \quad (20)$$

Eq. (20) imposes some limits to the observability of nonclassical effects on the cyclotron motion; in fact the added thermal noise should be much less than the cyclotron vacuum noise for the chosen frequency, i.e.  $\gamma_z K_B T \ll (\hbar k |\epsilon|)^2$ .

#### IV. THE CASE OF $\phi = 0$

Let us now consider the case of  $\phi = 0$ , and keeping only terms up to the second order in  $k\hat{z}$ , the Hamiltonian (10) reduces to

$$\begin{aligned} \hat{H} = & \hbar\omega_z \left( \hat{a}_z^\dagger \hat{a}_z + \frac{1}{2} \right) + \hbar\omega_c \left( \hat{a}_c^\dagger \hat{a}_c + \frac{1}{2} \right) \\ & + \hbar \left[ \epsilon^* \hat{a}_c e^{i\Omega t} + \epsilon \hat{a}_c^\dagger e^{-i\Omega t} \right] \left[ 1 - \frac{k^2 \hat{z}^2}{2} \right], \end{aligned} \quad (21)$$

which clearly shows the nonlinear coupling as a consequence of the higher order expansion with respect to the case of the previous Section.

Let us study the general case including losses. The latter are present in the axial degree of freedom once the connection with the external circuit is established, as pointed out in the previous Section. Instead, the noise on the cyclotron degree of freedom could arise e.g. from radiative damping (though it can be strongly reduced with an appropriate trap geometry).

Hence, by starting from the Hamiltonian (21), we obtain the following Quantum Stochastic Differential Equations

$$\frac{d\hat{a}_c}{dt} = -i\Delta\hat{a}_c - \frac{\gamma_c}{2}\hat{a}_c - i\epsilon(1 - \kappa^2\hat{Z}^2) + \sqrt{\gamma_c}\hat{a}_c^{in}, \quad (22)$$

$$\frac{d\hat{a}_c^\dagger}{dt} = i\Delta\hat{a}_c^\dagger - \frac{\gamma_c}{2}\hat{a}_c^\dagger + i\epsilon^*(1 - \kappa^2\hat{Z}^2) + \sqrt{\gamma_c}[\hat{a}_c^{in}]^\dagger, \quad (23)$$

$$\frac{d\hat{Z}}{dt} = \omega_z\hat{P}_z, \quad (24)$$

$$\frac{d\hat{P}_z}{dt} = -\omega_z\hat{Z} + 2\kappa^2(\epsilon^*\hat{a}_c + \epsilon\hat{a}_c^\dagger)\hat{Z} + f - \frac{\gamma_z}{m_0}\hat{P}_z - \Xi, \quad (25)$$

where  $\Delta = \omega_c - \Omega$ ,  $f$  is a driving term for the axial motion,  $\gamma_c$  the cyclotron damping constant, and  $\hat{a}_c^{in}$ ,  $\Xi$  are the noise terms (we shall consider the situation where only the vacuum contributes to the cyclotron noise). We have introduced the scaled variables  $\hat{Z} = \sqrt{m_0\omega_z/\hbar}\hat{z}$ ,  $\hat{P}_z = \sqrt{1/\hbar m_0\omega_z}\hat{p}_z$ ,  $\Xi = \sqrt{1/\hbar m_0\omega_z}\xi$ , and  $\kappa^2 = \hbar k^2/2m_0\omega_z$ . From the Eq. (25) we can see that the cyclotron quadrature causes a shift of the resonant frequency of the axial motion, so its indirect measurement results feasible.

The system of equations (22-25) can be linearized around the steady state [11]. The stationary values  $\bar{\alpha}_c$ ,  $\bar{Z}$  and  $\bar{P}_z$  can be obtained from the following equations

$$0 = -\left(\frac{\gamma_c}{2} + i\Delta\right)\bar{\alpha}_c - i\epsilon(1 - \kappa^2\bar{Z}^2), \quad (26)$$

$$0 = -\left(\frac{\gamma_c}{2} - i\Delta\right)\bar{\alpha}_c^* + i\epsilon^*(1 - \kappa^2\bar{Z}^2), \quad (27)$$

$$0 = \omega_z\bar{P}_z, \quad (28)$$

$$0 = -[\omega_z - 2\kappa^2(\epsilon^*\bar{\alpha}_c + \epsilon\bar{\alpha}_c^*)]\bar{Z} + f. \quad (29)$$

The linearized system is then

$$\frac{d}{dt} \begin{pmatrix} \hat{a}_c \\ \hat{a}_c^\dagger \\ \hat{Z} \\ \hat{P}_z \end{pmatrix} = \mathbf{M} \begin{pmatrix} \hat{a}_c \\ \hat{a}_c^\dagger \\ \hat{Z} \\ \hat{P}_z \end{pmatrix} + \begin{pmatrix} \sqrt{\gamma_c}\hat{a}_c^{in} \\ \sqrt{\gamma_c}[\hat{a}_c^{in}]^\dagger \\ 0 \\ -\Xi \end{pmatrix}, \quad (30)$$

where now the operators indicate the quantum fluctuations with respect to the steady state, and

$$\mathbf{M} = \begin{pmatrix} -\left(\frac{\gamma_c}{2} + i\Delta\right) & 0 & 2i\epsilon\kappa^2\bar{Z} & 0 \\ 0 & -\left(\frac{\gamma_c}{2} - i\Delta\right) & -2i\epsilon^*\kappa^2\bar{Z} & 0 \\ 0 & 0 & 0 & \omega_z \\ -2\epsilon^*\kappa^2\bar{Z} & -2\epsilon\kappa^2\bar{Z} & -\omega_z + 2\kappa^2(\epsilon^*\bar{\alpha}_c + \epsilon\bar{\alpha}_c^*) & -\frac{\gamma_z}{m_0} \end{pmatrix}. \quad (31)$$

The spectral matrix can be calculated as

$$\mathbf{S}(\omega) = (i\omega\mathbf{I} - \mathbf{M})^{-1}\mathbf{D}(-i\omega\mathbf{I} - \mathbf{M}^T)^{-1}, \quad (32)$$

where  $\mathbf{I}$  is the four by four identity matrix,  $\mathbf{M}^T$  means the transposed, and

$$\mathbf{D} = \begin{pmatrix} 0 & \gamma_c & 0 & 0 \\ 0 & 0 & 0 & 0 \\ 0 & 0 & 0 & 0 \\ 0 & 0 & 0 & \frac{\gamma_z}{m_0} N_{th} \end{pmatrix}, \quad (33)$$

with  $N_{th} = K_B T / \hbar \omega_z$  the number of thermal excitations.

The momentum correlation for the axial motion will be  $\mathbf{S}_{44}$ ; this quantity is plotted in Fig.1. The dashed line represents the resonance in absence of coupling and the solid line the resonance in presence of it. The separation between peaks is proportional to the cyclotron quadrature amplitude. So, it gives us an indirect value of that cyclotron observable.

Furthermore, the variance for the amplitude cyclotron quadrature is given by integrating the quantity  $\mathbf{S}_{11} + \mathbf{S}_{22} + \mathbf{S}_{12} + \mathbf{S}_{21}$ , and it is plotted in Fig.2 (dashed line). The same figure also shows the variance for the orthogonal quadrature (solid line). It can be seen that the system exhibits squeezing effects depending on the detuning. It is worth noting that such effects are not much sensitive to thermal noise.

The stability of the system, for the values of parameters used, is checked through the signs of the eigenvalues of the matrix  $\mathbf{M}$ .

In this Section and in the previous one we have shown that the terms beyond the dipole approximation could play an important role and should not be neglected abruptly. As a matter of fact we have presented a variety of effects (see e.g. Figs.1 and 2) that could be measured in common Penning traps.

To go further, in the following, we shall explore other possibilities.

## V. NONCLASSICAL STATES

We now demonstrate the generation of nonclassical effects due to the nonlinearity induced by Hamiltonian (21).

### A. The central resonance

If we tune the standing wave at frequency  $\Omega = \omega_c$ , and pass to the interaction picture, the Hamiltonian (21) simply becomes

$$\hat{H} = \sqrt{2}\hbar|\epsilon|\hat{X}_c \left[ 1 - \kappa^2 \left( \hat{a}_z^\dagger \hat{a}_z + \frac{1}{2} \right) \right], \quad (34)$$

where we have disregarded the rapidly oscillating terms  $\hat{a}_z^\dagger e^{-2i\omega_z t}$  and  $\hat{a}_z e^{2i\omega_z t}$  (i.e. we made the Rotating Wave Approximation).

Starting from initial coherent states for both modes

$$|\Psi(0)\rangle = |\alpha\rangle_c \otimes |\beta\rangle_z, \quad (35)$$

we obtain from the Hamiltonian (34) the following state at the time  $t$

$$|\Psi(t)\rangle = e^{-|\beta|^2/2} \sum_{n=0}^{\infty} \frac{\beta^n}{\sqrt{n!}} |\theta_n t\rangle_c \otimes |n\rangle_z, \quad (36)$$

where  $\theta_n = i\epsilon\kappa^2 n$ . In writing the state (36) we have disregarded, for the sake of simplicity, the quantity  $\alpha - i\epsilon(1 - \kappa^2/2)t$ , which is common to each cyclotron component (this corresponds to an overall displacement in the cyclotron phase space).

Therefore, the electron motion evolves classically as a mixture of coherent states. Thus, during the evolution, no nonclassical states of the electron are generated. However, because of the entanglement between the cyclotron and the axial degrees of freedom, it is possible to generate nonclassical states of the cyclotron motion by performing conditional

measurements on the axial degree of freedom. In particular, a measurement of the axial current corresponds to the projection onto an eigenstate  $|p_z\rangle$  of the axial momentum

$$|\Psi(t)\rangle_{after} = \mathcal{N} \sum_{n=0}^{\infty} \left[ e^{-|\beta|^2/2} \frac{\beta^n}{\sqrt{n!}} \langle p_z | n \rangle_z \right] |\theta_n t\rangle_c \otimes |p_z\rangle, \quad (37)$$

where  $\mathcal{N}$  is a normalization constant and  $\langle p_z | n \rangle_z$  are the harmonic oscillator wave functions in the momentum space. It is immediately seen from the above expression, that after the measurement the system is left in a superposition of coherent cyclotronic states which could have nonclassical features. Whenever the number of coherent states that are being superposed is small, the states are known as Schrödinger cat states [12].

It is worth noting that the separation between the superposed coherent states is given by  $|\epsilon|\kappa^2 t$ , and therefore it can be made truly macroscopic emphasizing the nonclassicality (by simply requiring that  $|\epsilon|\kappa^2 t > 1$ ). However, one has to be careful when satisfying the above condition, since it also implies a strong excitation of the cyclotron motion (the overall displacement that has been disregarded), which in turn could give rise to instabilities or even, the loss of the particle over the trap's walls.

The Wigner function of the cyclotron state generated by conditional measurement can be written as

$$W(Q, P) = \mathcal{N}^2 \sum_{m,n} c_m^* c_n \exp \left[ -Q^2 - P^2 - \frac{|\zeta_m|^2}{2} - \frac{|\zeta_n|^2}{2} + \sqrt{2}Q(\zeta_n + \zeta_m^*) - \sqrt{2}iP(\zeta_n - \zeta_m^*) - \zeta_n \zeta_m^* \right], \quad (38)$$

where the variable  $Q, P$  are associated to the quadratures  $\hat{X}_{\varphi=0}$  and  $\hat{X}_{\varphi=\pi/2}$  respectively, and

$$c_n = e^{-|\beta|^2/2} \frac{\beta^n}{\sqrt{n!}} \langle p_z | n \rangle_z, \quad (39)$$

$$\zeta_n = \theta_n t. \quad (40)$$

In Fig. 3 we present the Wigner function of the cyclotron state generated by conditional measurement on the axial degree of freedom. The negative parts and several oscillations show the nonclassicality of such a state.

We have considered the measurement process conditioning the cyclotron state as instantaneous, however, it always takes a finite time during which the system undergoes the back-action of the measurement apparatus. To take into account these effects we should adopt a precise Hamiltonian model describing the measurement of the observable  $\hat{p}_z$ . Nevertheless, from a phenomenological point of view, we can model the measurement process, performed on the state  $\hat{\rho}(t) = |\Psi(t)\rangle\langle\Psi(t)|$ , during a time  $\tau$ , as the transition

$$\hat{\rho}(t) \rightarrow \text{Tr}_z [\hat{\rho}(t + \tau) |p_z\rangle\langle p_z|], \quad (41)$$

where  $\hat{\rho}(t + \tau)$  is obtained from  $\hat{\rho}(t)$  through free evolution in a thermal bath (representing the back-action of the measurement apparatus on the system), while the projector indicates the output resulting at the end of the measurement [13].

To evaluate the effects of the measurement on the cyclotron state we should calculate the reduced density operator (r.h.s. of Eq.(41)). Its corresponding Wigner function is derived in Appendix A as

$$W(Q, P, \tau) = \mathcal{N}^2 \sum_{m,n} \frac{\beta^m (\beta^*)^n}{m! n!} 2^{-(m+n)/2} I_{m,n} \exp \left[ -Q^2 - P^2 - \frac{|\zeta_m|^2}{2} - \frac{|\zeta_n|^2}{2} + \sqrt{2}Q(\zeta_m + \zeta_n^*) - \sqrt{2}iP(\zeta_m - \zeta_n^*) - \zeta_m \zeta_n^* \right], \quad (42)$$

where

$$I_{m,n} = 2^n m! \int dv \exp \left\{ - [e^{-2\Gamma\tau} + 2N_{th}(1 - e^{-2\Gamma\tau})] v^2 - 2iP_z v \right\} \times (-ve^{-\Gamma\tau})^{n-m} L_m^{n-m}(2v^2 e^{-2\Gamma\tau}); \quad n > m, \quad (43)$$

with  $L_m^n$  the associated Laguerre polynomials, and  $\Gamma = \gamma_z/m_0$  the effective axial damping constant.

The Wigner function (42) is plotted in Fig.4 and shows the deleterious effects of finite time measurement on the nonclassical state represented in Fig.3. Of course, these effects strongly depend on the number of thermal excitations  $N_{th}$  as well.

Once the cat states are generated by the conditional measurements, it would be possible to detect them by using indirect measurements as proposed in the previous Sections.

## B. The sideband resonance

We now return to the Hamiltonian (21) to consider another resonance, in this case  $\Omega = (\omega_c - 2\omega_z) - \delta$ , where  $\delta$  is a small detuning (i.e.  $\delta \ll \omega_z$ ) introduced for convenience. In a frame rotating at frequency  $\omega_c - \delta$ , we then have

$$\hat{H} = \hbar\delta\hat{a}_c^\dagger\hat{a}_c - \hbar\frac{|\epsilon|\kappa^2}{2}(\hat{a}_c\hat{a}_z^{\dagger 2}e^{-i\varphi} + \hat{a}_c^\dagger\hat{a}_z^2e^{i\varphi}). \quad (44)$$

This is a trilinear Hamiltonian analogous to that studied in nonlinear optical processes like parametric oscillation or second harmonic generation [11].

The equations of motion are

$$\frac{d\hat{a}_c}{dt} = -i\delta\hat{a}_c + i\frac{1}{2}|\epsilon|\kappa^2\hat{a}_z^2, \quad (45)$$

$$\frac{d\hat{a}_z}{dt} = i|\epsilon|\kappa^2\hat{a}_z^\dagger\hat{a}_c; \quad (46)$$

and, by adiabatic elimination of the cyclotron mode, we get

$$\frac{d\hat{a}_z}{dt} = i\frac{|\epsilon|^2\kappa^4}{2\delta}\hat{a}_z^\dagger\hat{a}_z^2. \quad (47)$$

This equation corresponds to an effective Hamiltonian for the axial motion of the type

$$\hat{H}_{eff} = -\hbar\frac{|\epsilon|^2\kappa^4}{4\delta}(\hat{a}_z^\dagger)^2\hat{a}_z^2, \quad (48)$$

which shows a well known Kerr-type nonlinearity. Hence, we should expect nonclassical effects, such as Schrödinger cat states, when one starts from the initial conditions (35), also in the axial mode. In fact, the evolved axial state can be written as

$$|\psi(t)\rangle_z = \exp[iG((\hat{a}_z^\dagger\hat{a}_z)^2 - \hat{a}_z^\dagger\hat{a}_z)t]|\beta\rangle_z, \quad G = \frac{|\epsilon|^2\kappa^4}{4\delta}. \quad (49)$$

It is easy to show that after a time  $t = \pi/(2G)$  the initial coherent state evolves into a cat state of the type discussed in Ref. [14]

$$|\psi(t = \pi/(2G))\rangle = \frac{1}{\sqrt{2}}\left[e^{-i\pi/4}| -i\beta\rangle + e^{i\pi/4}|i\beta\rangle\right]. \quad (50)$$

That state shows interference in the phase space which could be detected by measuring an appropriate quadrature. Therefore, by adjusting the initial conditions we may exploit the axial momentum measurement to see such interference. The Wigner function of the state (50) results

$$\begin{aligned} W(Z, P_z) &= \frac{1}{\pi}e^{-|\beta|^2 - Z^2 - P_z^2} \\ &\times \left\{ e^{-|\beta|^2} \cosh\left[2\sqrt{2}P_z \operatorname{Re}(\beta) - 2\sqrt{2}Z \operatorname{Im}(\beta)\right] \right. \\ &\left. + e^{|\beta|^2} \sin\left[2\sqrt{2}P_z \operatorname{Im}(\beta) + 2\sqrt{2}Z \operatorname{Re}(\beta)\right] \right\}, \quad (51) \end{aligned}$$

and is represented in Fig.5. The fact that only two coherent states are being superposed is evident from the two hills besides the central structure, differently from the situation of Fig.3 where more components contributes to the cat state.

Of course, we should deal again with the problem of measurement, whose process renders the system open, hence, the dissipation tends to wash out the nonclassical effects. To evaluate this phenomenon we assume to switch off the nonlinearity at the time of cat generation, and a subsequent free evolution of the axial degree of freedom in a thermal bath, representing the effects of the external readout circuit. If the latter takes a time  $\tau$ , we have (see Appendix B)

$$W(Z, P_z, \tau) = \frac{1}{2} e^{-|\beta|^2 + \beta^2/2 + \beta^{*2}/2} \left\{ e^{2\text{Im}(\beta)^2} [I_1 + I_2] - i e^{-2\text{Re}(\beta)^2} [I_3 - I_4] \right\}, \quad (52)$$

where

$$I_i = \frac{2}{\pi \sqrt{4\mathcal{A}\mathcal{B} - \mathcal{C}^2}} \exp \left[ \frac{\mathcal{B}\mathcal{D}_i^2 + \mathcal{C}\mathcal{D}_i\mathcal{E}_i + \mathcal{A}\mathcal{E}_i^2}{4\mathcal{A}\mathcal{B} - \mathcal{C}^2} \right]; \quad i = 1, 2, 3, 4, \quad (53)$$

with

$$\mathcal{A} = \frac{1}{\Gamma^2} (e^{-\Gamma\tau} - 1)^2 + 1 \quad (54)$$

$$+ 2 \frac{N_{th}}{\Gamma^2} (1 - e^{-2\Gamma\tau}) - 8 \frac{N_{th}}{\Gamma^2} (1 - e^{-\Gamma\tau}) + 4 \frac{N_{th}}{\Gamma} \tau;$$

$$\mathcal{B} = e^{-2\Gamma\tau} + 2N_{th}(1 - e^{-2\Gamma\tau}); \quad (55)$$

$$\mathcal{C} = -\frac{2}{\Gamma} e^{-\Gamma\tau} (e^{-\Gamma\tau} - 1) - 4 \frac{N_{th}}{\Gamma} (1 - e^{-2\Gamma\tau}) + 8 \frac{N_{th}}{\Gamma} (1 - e^{-\Gamma\tau}); \quad (56)$$

and

$$\mathcal{D}_2 = \mp 2\sqrt{2}i\text{Im}(\beta) \mp \frac{\sqrt{2}}{\Gamma} i\text{Re}(\beta)e^{-\Gamma\tau} \pm \frac{\sqrt{2}}{\Gamma} i\text{Re}(\beta) + 2iZ; \quad (57)$$

$$\mathcal{D}_4 = \mp 2\sqrt{2}\text{Re}(\beta) \pm \frac{\sqrt{2}}{\Gamma} \text{Im}(\beta)e^{-\Gamma\tau} \mp \frac{\sqrt{2}}{\Gamma} \text{Im}(\beta) + 2iZ; \quad (58)$$

$$\mathcal{E}_2 = \mp 2\sqrt{2}i\text{Re}(\beta)e^{-\Gamma\tau} - 2iP_z; \quad (59)$$

$$\mathcal{E}_4 = \pm 2\sqrt{2}\text{Im}(\beta)e^{-\Gamma\tau} - 2iP_z. \quad (60)$$

The Wigner function (52) is plotted in Fig.6 and shows that the cat state (50) is very sensitive to the noise induced by the measurement.

## VI. CONCLUSIONS

In conclusion, we have studied a trapped electron interacting with a standing radiation field and have shown that several interesting features can arise when the dipole approximation is not invoked. First, the proposed model provide a method for indirect measurement on the cyclotron degree of freedom. On the other hand, the possibilities to generate nonclassical states could be useful to test the linearity of Quantum Mechanics [16], as well as to probe the decoherence of a mesoscopic system [17]. Furthermore, it is worth noting that the entanglement induced by the radiation field could also be used to explore the quantum logic possibilities of a trapped electron system.

Hence, the geonium system in such configuration could result alternative and/or complementary to other trapped systems. In addition it has the advantage of involving a structureless particle, while for example an ion in a Paul trap behaves as a two-level system only ideally. Moreover, having the electron an antiparticle, the model could also be used to perform some fundamental tests of simmetry.

Finally, based on these considerations we conclude that it should be an interesting challenge to experimentally implement this model. The realistic values of parameters (see e.g. Ref. [5]) we have used yield that feasible with the actual technology. The main problem could be represented by the low values of  $N_{th}$  in Sec. IV, however, to better evidenciate the desired effects one could adjust the experimental set up in order to increase the dishomegeneity of the field experienced by the particle (to this end, we note that traps bigger than the usual are available as well [18]).

## APPENDIX A

We consider the position space matrix elements of the state  $\hat{\rho}(t)$ , i.e.

$${}_c\langle Q + Y | {}_z\langle Z' | \hat{\rho}(t) | Z'' \rangle_z | Q - Y \rangle_c, \quad (61)$$

and we denote them as  $\wp(Z', Z'')$  since the evolution will take place only in the axial space. The dependence on the cyclotron variables remains implicit. Then, with the aid of Eq. (36) we get

$$\wp(Z', Z'') = \sum_{m,n} C_m C_n^* \exp \left[ - \left( Z'^2 + Z''^2 \right) / 2 \right] H_m(Z') H_n(Z''), \quad (62)$$

where  $H_m$  are the Hermite polynomials, and

$$C_m = \left( \frac{1}{\pi} \right)^{1/4} \frac{1}{\sqrt{2^m m!}} e^{-|\beta|^2/2} \frac{\beta^m}{\sqrt{m!}} \langle Q + Y | \zeta_m \rangle, \quad (63)$$

$$C_n^* = \left( \frac{1}{\pi} \right)^{1/4} \frac{1}{\sqrt{2^n n!}} e^{-|\beta|^2/2} \frac{(\beta^*)^n}{\sqrt{n!}} \langle \zeta_n | Q - Y \rangle. \quad (64)$$

The master equation for the free evolution in a thermal bath [15] has the corresponding partial differential equation for the probability  $\wp$

$$\begin{aligned} \partial_\tau \wp(Z', Z'', \tau) = & \left\{ \frac{i}{2} \left( \frac{\partial^2}{\partial Z'^2} - \frac{\partial^2}{\partial Z''^2} \right) - \frac{\Gamma}{2} (Z' - Z'') \left( \frac{\partial}{\partial Z'} - \frac{\partial}{\partial Z''} \right) \right. \\ & \left. - \Gamma N_{th} (Z' - Z'')^2 \right\} \wp(Z', Z'', \tau), \end{aligned} \quad (65)$$

where we have set  $\Gamma = \gamma_z/m_0$ . Both, the damping constant and the time are scaled by the axial frequency, i.e.  $\Gamma/\omega_z \rightarrow \Gamma$  and  $\tau\omega_z \rightarrow \tau$ .

The differential equation (65) is considerably simplified by the change of variables

$$Z' = u + v, \quad (66)$$

$$Z'' = u - v, \quad (67)$$

leading to

$$\partial_\tau \wp(u, v, \tau) = \left\{ \frac{i}{2} \frac{\partial^2}{\partial u \partial v} - \Gamma v \frac{\partial}{\partial v} - 4\Gamma N_{th} v^2 \right\} \wp(u, v, \tau). \quad (68)$$

By using the Fourier transform

$$\wp(u, v) = \int dq e^{2iqu} \tilde{\wp}(q, v), \quad (69)$$

Eq. (68) becomes

$$\frac{\partial \tilde{\wp}}{\partial \tau} + (q + \Gamma v) \frac{\partial \tilde{\wp}}{\partial v} = -4\Gamma N_{th} v^2 \tilde{\wp}, \quad (70)$$

which can be solved by the method of characteristics. The solution takes the form

$$\begin{aligned} \tilde{\wp}(q, v, \tau) = & \tilde{\wp} \left( q, \left[ \left( v + \frac{q}{\Gamma} \right) e^{-\Gamma\tau} - \frac{q}{\Gamma} \right], 0 \right) \\ & \times \exp \left\{ -2N_{th} \left( v + \frac{q}{\Gamma} \right)^2 (1 - e^{-2\Gamma\tau}) \right. \\ & \left. + \frac{8N_{th}}{\Gamma} q \left( v + \frac{q}{\Gamma} \right) (1 - e^{-\Gamma\tau}) \right\} e^{-4q^2 N_{th} \tau / \Gamma}. \end{aligned} \quad (71)$$

In our case, from the Eqs. (62), (66), (67), (69), results

$$\begin{aligned} \tilde{\varphi}(q, v, 0) &= \sqrt{\pi} \exp[-v^2 - q^2] \\ &\times \left\{ \sum_{m < n} C_m C_n^* 2^n m! (-v - iq)^{n-m} L_m^{n-m} [2(v^2 + q^2)] \right. \\ &+ \sum_{m=n} |C_n|^2 2^n n! L_m [2(v^2 + q^2)] \\ &\left. + \sum_{m > n} C_m C_n^* 2^m n! (-v - iq)^{m-n} L_n^{m-n} [2(v^2 + q^2)] \right\}, \end{aligned} \quad (72)$$

where  $L_n^m$  indicates the associated Laguerre polynomials. Therefore, starting from the above expression, the solution (71) can be easily constructed.

The Wigner function of the cyclotron state after a measurement giving the result  $p_z$  (or equivalently  $P_z$ ), will be

$$W(Q, P, \tau) = \mathcal{N}^2 \int dY {}_c\langle Q + Y | {}_z\langle P_z | \hat{\rho}(t + \tau) | P_z \rangle_z | Q - Y \rangle_c e^{-2iPY}, \quad (73)$$

where  $\mathcal{N}$  is the normalization constant needed after the projection. By inserting identities in terms of the set of states  $\{|u \pm v\rangle_z\}$ , and with the aid of the Fourier transform (69), we get

$$W(Q, P, \tau) = \mathcal{N}^2 \int dY \int dv \tilde{\varphi}(0, v, \tau) e^{-2ivP_z - 2iYP}. \quad (74)$$

The dependence on the cyclotron variables  $Q$  and  $Y$  is implicit on  $\varphi$ . Hence, by performing the integration one arrives at the expression (42).

## APPENDIX B

If  $\tau$  is the duration of the measurement, at the end of the measurement we have

$$W(Z, P_z, \tau) = \frac{1}{\pi} \int dv \langle Z + v | \hat{\rho}_z(\tau) | Z - v \rangle e^{-2iP_z v}, \quad (75)$$

$$= \frac{1}{\pi} \int dv \varphi(Z, v, \tau) e^{-2iP_z v}, \quad (76)$$

$$= \frac{1}{\pi^2} \int dv \int dq \tilde{\varphi}(q, v, \tau) e^{-2iP_z v + 2iqZ}, \quad (77)$$

where  $\tilde{\varphi}(q, v, \tau)$  is the same of Eq. (71), but with the initial condition determined by Eq.(50)

$$\begin{aligned} \tilde{\varphi}(q, v, 0) &= \frac{1}{2} e^{-|\beta|^2 - q^2 - v^2 + \beta^2/2 + \beta^{*2}/2} \\ &\times \left\{ \exp \left[ 2\text{Im}(\beta)^2 - 2\sqrt{2}i\text{Im}(\beta)q - 2\sqrt{2}i\text{Re}(\beta)v \right] \right. \\ &+ \exp \left[ 2\text{Im}(\beta)^2 + 2\sqrt{2}i\text{Im}(\beta)q + 2\sqrt{2}i\text{Re}(\beta)v \right] \\ &- i \exp \left[ -2\text{Re}(\beta)^2 - 2\sqrt{2}\text{Re}(\beta)q + 2\sqrt{2}\text{Im}(\beta)v \right] \\ &\left. + i \exp \left[ -2\text{Re}(\beta)^2 + 2\sqrt{2}\text{Re}(\beta)q - 2\sqrt{2}\text{Im}(\beta)v \right] \right\}. \end{aligned} \quad (78)$$

Thus, performing the double integral in Eq.(77) we get the expression (52).

## ACKNOWLEDGMENTS

A.M.M. would like to thank the University of Camerino for the kind hospitality. S.M. would like to thank the Istituto Superior Técnico for the kind hospitality and the INFN (Sezione Perugia) for partial support.

---

- [1] W. Paul, *Rev. Mod. Phys.* **62**, 531 (1990).
- [2] See e.g. lectures by C. Cohen-Tannoudji and W. D. Phillips on laser cooling of neutral atoms and lectures by H. Walther and R. Blatt on laser cooling of trapped ions, in *Fundamental Systems in Quantum Optics*, 1990 Les Houches Session n. LIII, edited by J. Dalibard, J. M. Raimond and J. Zinn-Justin (North-Holland, Amsterdam, 1992).
- [3] F. M. Penning, *Physica (Amsterdam)* **3**, 873 (1936).
- [4] R. S. Van Dyck Jr., P. B. Schwinberg and H. G. Dehmelt, in *Atomic Physics 9*, edited by R. S. Van Dyck Jr. and E. N. Fortson (World Scientific, Singapore, 1984).
- [5] L. S. Brown and G. Gabrielse, *Rev. Mod. Phys.* **58**, 233 (1986).
- [6] I. Marzoli and P. Tombesi, *Europhys. Lett.* **24**, 515 (1993).
- [7] S. Mancini and P. Tombesi, *Phys. Rev. A* **56**, R1679 (1997).
- [8] G. Gabrielse, H. Dehmelt and W. Kells, *Phys. Rev. Lett.* **54**, 537 (1985).
- [9] There can be some limiting conditions on the existence of such waves due to the trap electrodes, however one can develop the same theory for other geometries, like cylindrical traps (see e.g. G. Gabrielse and J. Tan in *Cavity Quantum Electrodynamics*, P. R. Berman Ed., Academic Press, London, 1994)
- [10] S. Mancini and P. Tombesi, *Phys. Rev. A* **56**, 3060 (1997).
- [11] see e.g. D. F. Walls and G. J. Milburn, *Quantum Optics*, (Springer, Berlin, 1994).
- [12] E. Schrödinger, *Naturwissenschaft.* **23**, 807 (1935); **23**, 823 (1935); **23**, 844 (1935).
- [13] The projector in Eq.(41) should be in reality, a projector on an interval of values for  $p_z$  which accounts for the uncertainty arising by relating the electric current at readout circuit with the axial observable. However, here for simplicity, we are not considering the dynamics of the readout apparatus (a detailed treatment of this subject in terms of input-output theory is given by I. Marzoli, Master Thesis, University of Camerino, 1992).
- [14] B. Yurke and D. Stoler, *Phys. Rev. Lett.* **57**, 13 (1986).
- [15] C. W. Gardiner, *Quantum Noise*, (Springer, Berlin, 1991).
- [16] S. Weinberg, *Phys. Rev. Lett.* **62**, 485 (1989).
- [17] W. H. Zurek, *Phys. Today* **44**, 36 (1991).
- [18] see e.g. J. Eades *et al.*, CERN Report No. PSSC/89-15 PSSC/P **118**, (1989).

#### FIGURE CAPTIONS

Fig.1 Spectrum of axial momentum for  $\Delta = 1.5 \times 10^4 \text{ s}^{-1}$ ,  $\kappa^2 = 10^{-6}$ ,  $\gamma_c = 1.5 \text{ s}^{-1}$ ,  $\gamma_z/m_0 = 20 \text{ s}^{-1}$ ,  $|\epsilon| = 1.4 \times 10^4 \text{ s}^{-1}$ ,  $\varphi = 3\pi/4$ ,  $f = 10^{11} \text{ s}^{-1}$ , and  $N_{th} = 10^3$ . The peak on the right represents the resonance in absence of coupling. The separation between peaks is proportional to the cyclotron quadrature amplitude.

Fig.2 Variance for the cyclotron quadratures  $X_{\varphi=0}$  (dashed line) and  $X_{\varphi=\pi/2}$  (solid line) as function of the detuning  $\Delta$ . The values of other parameters are the same of Fig.1.

Fig.3 The Wigner function of Eq. (38) is plotted for the parameters  $\beta = 1$ ,  $\epsilon\kappa^2 t = -2.4i$ , after an axial momentum measurement yielding the most probable value of  $p_z$ .

Fig.4 The same of Fig.3 including the effects of finite time measurement. Here  $\Gamma\tau = 0.1$  and  $N_{th} = 10$ .

Fig.5 The Wigner function of cat state (50) is plotted for  $\beta = 2$ .

Fig.6 The same of Fig.5 including the effects of finite time measurement. Here  $\Gamma = 6$ ,  $\tau = 0.4$ , and  $N_{th} = 10$ .

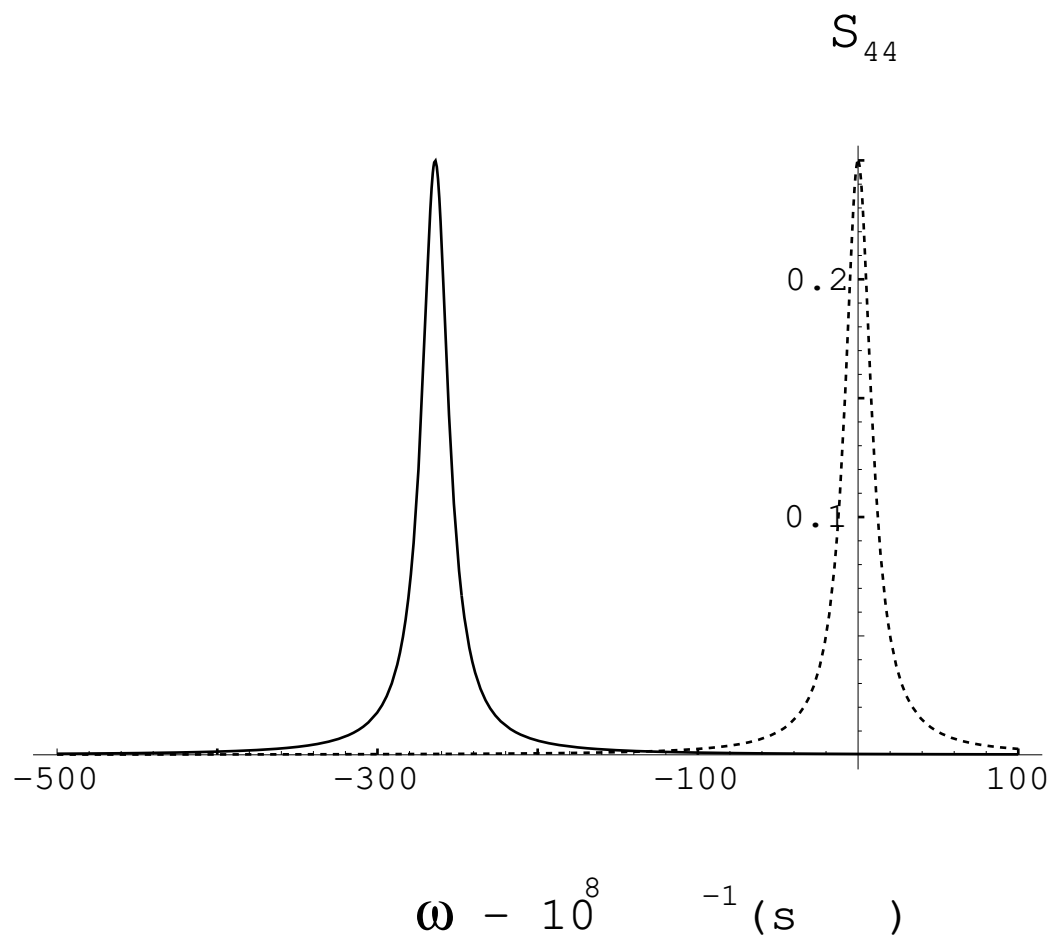


Fig.1 A. M. Martins et al.  
Electron-radiation.....

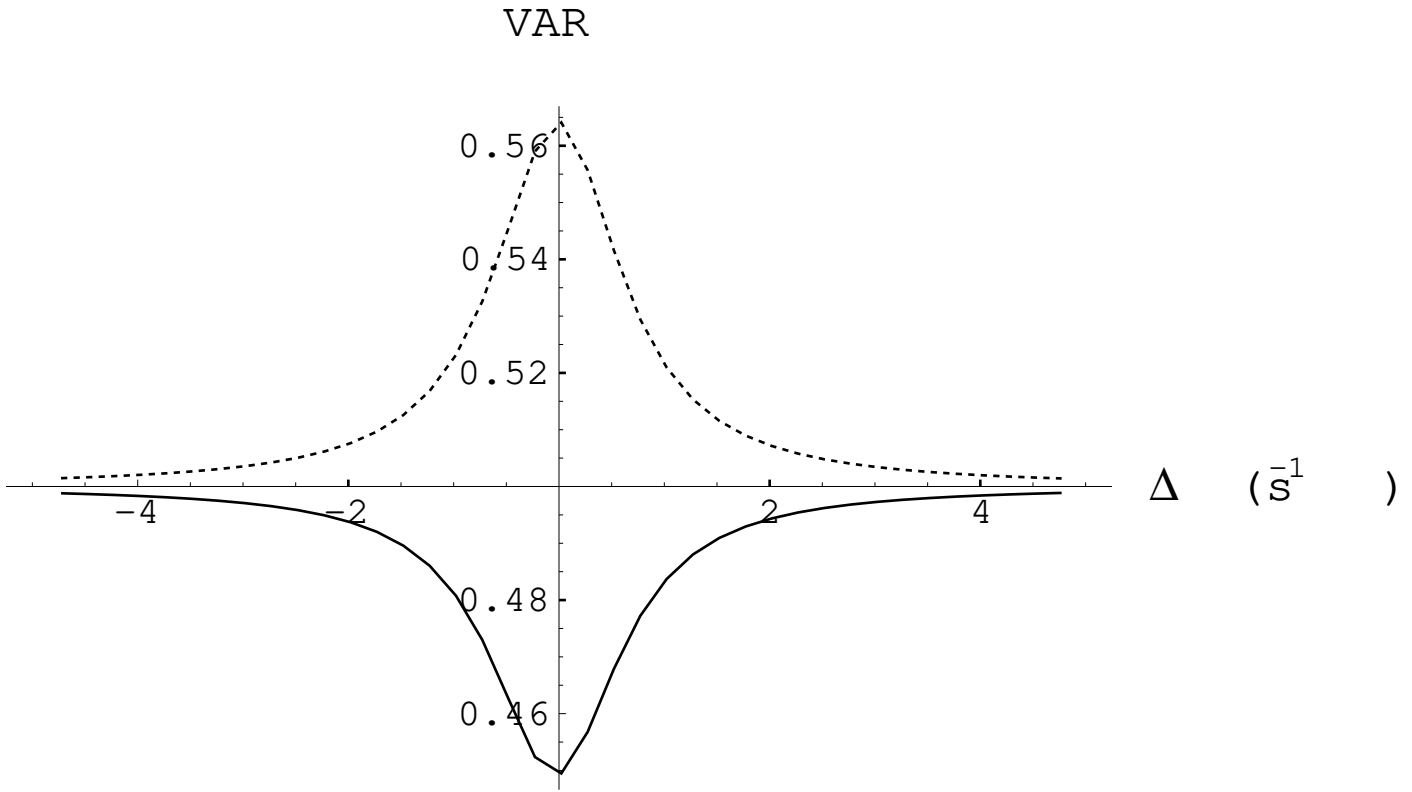


Fig.2 A. M. Martins et al.  
Electron-radiation.....

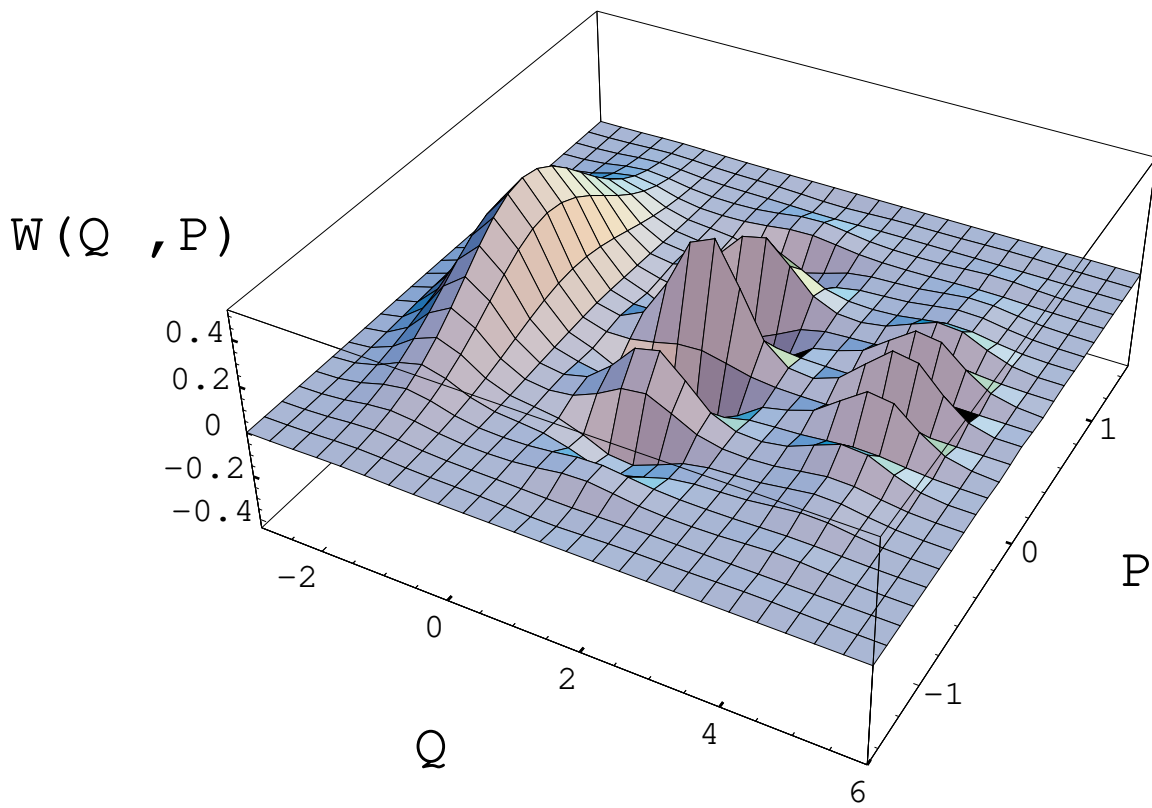


Fig.3 A. M. Martins et al.  
Electron-radiation.....

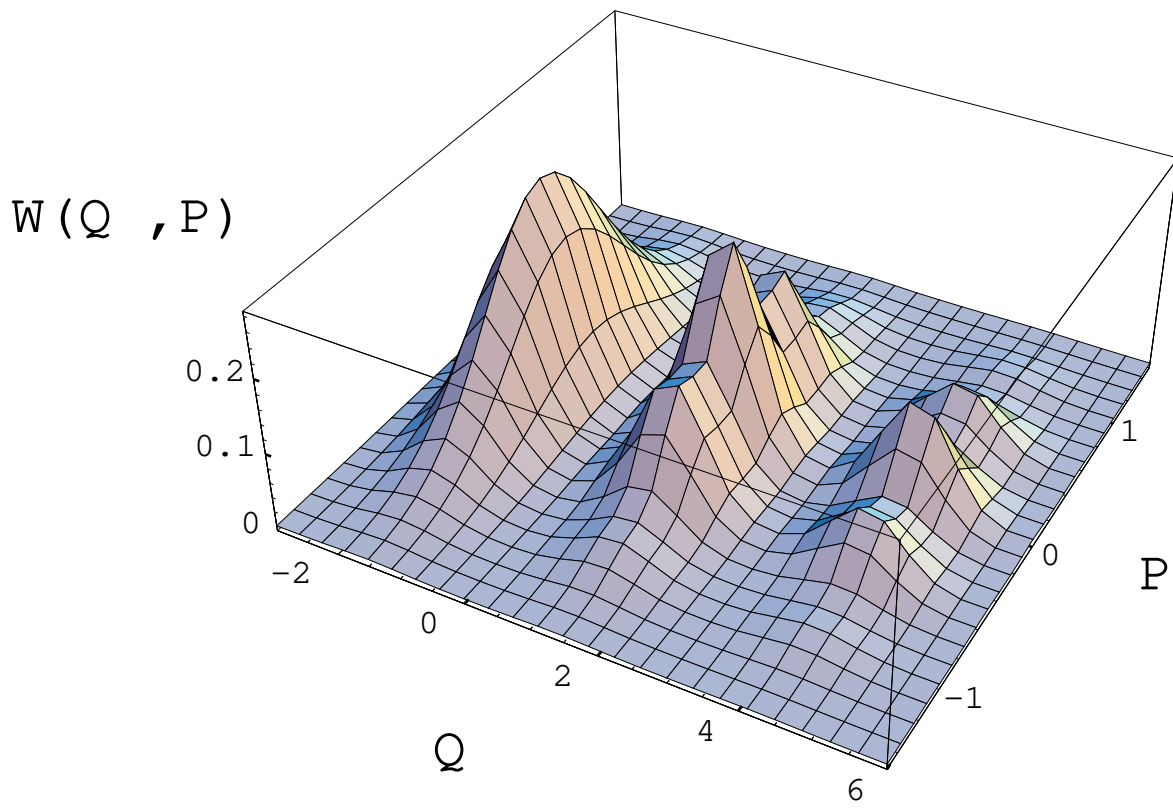


Fig.4 A. M. Martins et al.  
Electron-radiation.....

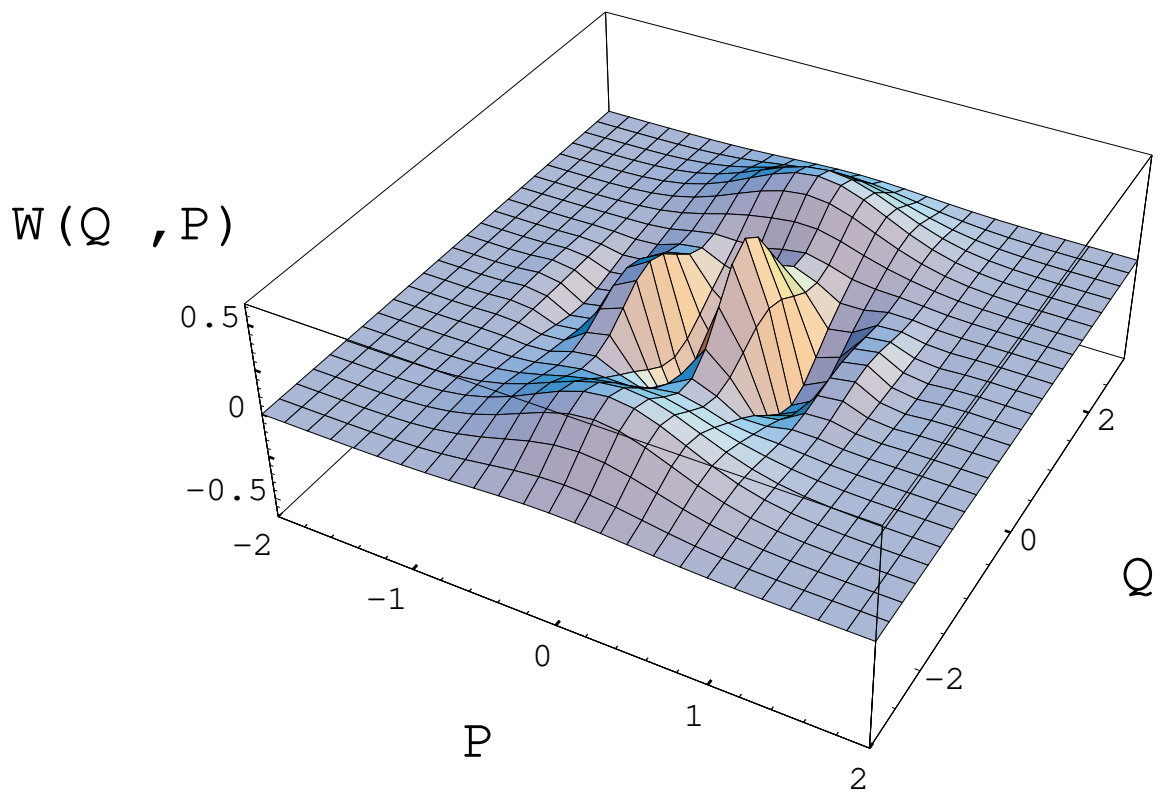


Fig.5 A. M. Martins et al.  
Electron-radiation.....

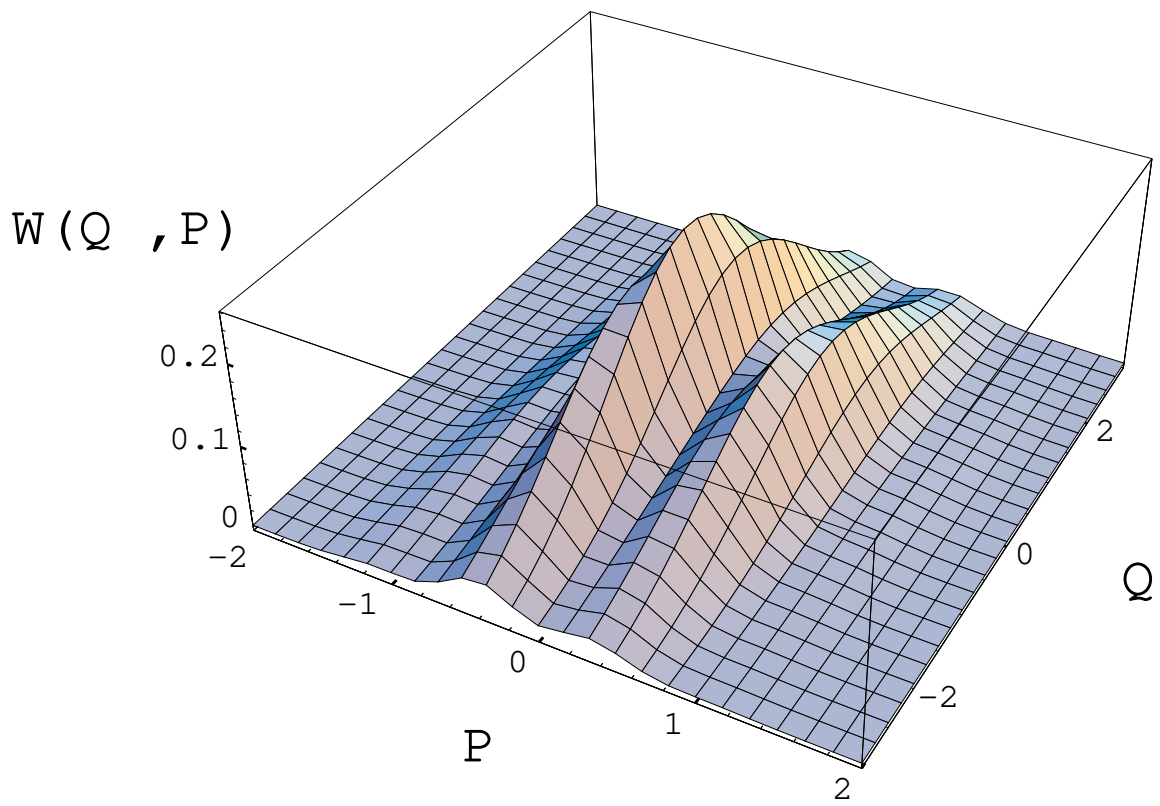


Fig.6 A. M. Martins et al.  
Electron-radiation.....